Journal of Hazardous Materials, 22 (1989) 85–100
Elsevier Science Publishers B.V., Amsterdam — Printed in The Netherlands

WIND EFFECTS ON DIFFUSION FLAMES OF FIRES OF HIGH SOURCE MOMENTUM

D.M. DE FAVERI, A. VIDILI*, R. PASTORINO and G. FERRAIOLO

Institute of Science and Technology of Chemical Engineering, University of Genoa, Via Opera Pia 15, 16145 Genoa (Italy)

(Received May 14, 1987; accepted in revised form March 2, 1989)

Summary

An experimental study has been carried out in a wind tunnel in order to provide exact correlations for predicting flame length of fires of high source momentum.

It has been shown that the length of laminar flames of fires of high source momentum ($Q^* > 1$) is effected not only by the source Froude number but also by the source Reynolds number if the Froude number is larger than 0.1.

On the other hand, the effect of the Reynolds number on the flame length is negligible if the Froude number is less than 0.1.

Furthermore, by adopting Sliepcevich's theoretical analysis (Ref. 1) on the angle of flame tilt due to the wind, this work provides two simple and practical equations which allows assessment of the angle of flame tilt due to wind for both conical and cylindrical shaped flames.

Introduction

Various authors [1–10] have given correlations or suggested guidelines for predicting the length of diffusion flames for fires with low source momentum ($Q^* < 1$ or $Q^* \sim 1$), with

$$Q^* = \frac{Q}{\rho_a T_a C_p g^{1/2} D^{5/2}} \quad , \tag{1}$$

where Q denotes the heat release (assuming efficient combustion) in kJ/s, ρ_a the air density in kg/m^3, T_a the air temperature in K, C_p the specific heat of air at constant pressure in kJ/kg K, g the gravitational acceleration constant in m/s^2, and D is the flame diameter in m.

The dimensionless ratio Q^* was introduced by Zukoski et al. [2] to represent the relative contribution of source momentum and flame buoyancy in fires.

Thomas et al. [3] presented dimensional arguments to show that flame length is governed by this ratio and that

$$(L/D) \propto (Q^{*2})^{1/(2p+1)} \tag{2}$$

*Present address: Montefluos S.p.A., Ausimont group, Via Principe Eugenio 1/5, 20155 Milano (Italy).

0304-3894/89/$03.50

where p is a representation of the flame shape factor varying from 0 to 2 for fires with increasing L/D (length-to-diameter ratio).

Cox and Chitty [4] reported in a study on a 0.3 m square burner for the heat release rates a range from 14 to 47 kW ($Q^* \sim 0.3$–0.9), and for the heat release rate per unit area (heatflux) 160–520 kW/m^2, where $L/D = 3.3\, Q^{*2/5}$.

This empirical result is similar to those published by other workers [2,5] even up to the 15.2 m diameter fires of JP4 fuel ($Q^* \sim 0.66$) reported by Raj [6] ($L \sim 45.7$ m).

It had been the intention on completion of the earlier work [4] that Cox and Chitty presented a further work [7] on a 0.6 m square burner for heat release rates ranging from 45 to 118 kW ($Q^* \sim 0.13$–0.28) and heat fluxes of 127–327 kW/m^2, where $L/D = 15.1\, Q^{*2}$ for $0.13 < Q^* < 0.28$.

The aforementioned authors also performed experimental tests on a 0.45 m square burner [7] ($0.28 < Q^* < 0.55$) and their data suggested the following relationship

$$L/D = 3.2\, Q^* \quad \text{for} \quad 0.28 < Q^* < 0.55 \quad .$$

The data presented by Cox and Chitty [7] for Q^* between 0.13 and 0.55 are both lower in magnitude and diverge from Zukoski's measurements [2] (for Q^* between 0.18 and 0.4) and Heskestad's suggested correlation [8] with decreasing Q^*.

The authors thought that the differences might have depended on burner shape. They carried out their tests with square burners while Zukoski's experiments were done with circular ones.

Cox and Chitty then observed that square burners produce shorter flames than circular ones perhaps because of the extra mixing induced at the corners. Furthermore the measurement technique employed is known to produce differences in flame length determination (up to 15% according to Cetegen et al. [9]).

In order to allow comparison with studies on circular sources the data presented in this work has been obtained by carrying out experimental tests by means of bowls.

The paper by Becker and Liang [5] presents general correlations for predicting flame length from the forced convection to the natural convection range.

In particular, the above authors studied free turbulent diffusion flames produced by a gas burner. They also re-examined the data of Blinov and Khudiakov [10] ($Q^* > 0.3$) and suggested a flame length square law dependence ($L/D \propto Q^{*2}$) for $L/D < 4.5$ and for a characteristic Reynold's number of $Re_L > 2500$, where

$$Re_L = 0.18 \left(\frac{g L^3}{\nu_a^2} \right)^{\frac{1}{2}} \tag{3}$$

The quantity gL^3/ν_a^2 is the effective-flame Grashoff number (ν_a is the kinematic viscosity of air).

Blinov and Khudiakov's experimental data [10] refer to flames in the natural convection limit.

In previous work [11] we presented a study on diffusion flames of fires of high source momentum which showed that the Froude number (u^2/gD) effects the flame length significantly.

In particular, the length-to-diameter ratio of the flame, L/D, decreases as the source Froude number is increased.

The previous work [11] assumed the generally accepted hypothesis that the Reynolds number (uD/ν_a) has little influence on flame extent.

The main aim of this study is to assess the real contribution of source Reynolds number on flame length of fires of high source momentum.

This study shows that under particular conditions the Reynolds number plays a significant effect on diffusion flame length.

Diffusion flames for fires of high source momentum have been observed in wind tunnel experiments in order to determine the extent of flame size and bending due to wind.

The experimental results have been correlated through the use of a simple physical model for the gross flame structure (see Fig. 1).

Wind tunnel experiments

Laboratory-scale tests of free burning pools of liquid were performed in a wind tunnel using Diesel fuel and a mixture of lubricant oil with exhausted Diesel.

The main parameters of the experiments are shown in Table 1.

Flame buoyancy was varied by using bowls with different diameters and different quantities of fuel inside the containers. Bowls were lain low in a pit, while their upper edges were flush with the bottom of wind tunnel.

Fuel vapor was lit after preheating the liquid with a bunsen burner, positioned just outside the wind tunnel under the bowl (see Fig. 1). After reaching the fire point, the warming of the fuel was stopped by shutting off the bunsen burner.

Conical-shaped flames were observed for all experimental runs. Flame length and inclination were measured through a glass window from where flame extent could be observed.

The flame extent was taken perpendicularly from the centre of the pool to the flame tip (see L and θ in Fig. 1).

Flame length and inclination maintained a steady value during every test.

A gradient of wind speed from the bottom to the top of wind tunnel was observed.

After measuring the wind speed at two different heights, the real wind speed

TABLE 1

Range of the main geometric and operational parameters used for wind tunnel experiments — Burning fuel characteristics

Wind tunnel characteristics	
Height	1.00 m
Width	1.20 m
Length	6.00 m
Thermal condition in wind tunnel: neutral to isothermal	
Operational parameters	
Wind speed: $0.191 \leqslant u \leqslant 0.891$ m/s	
Diameters of pools $3.66 \leqslant D \leqslant 10.9$ cm	
Dimensionless numbers	
Froude	$0.059 \leqslant Fr \leqslant 2.2$
Reynolds	$559 \leqslant Re \leqslant 5270$
Q^* (eqn. 1)	$3.8 \leqslant Q^* \leqslant 6.7$
Re_L (eqn. 3)	$2190 \leqslant Re_L \leqslant 6270$
L/D	$2.4 \leqslant L/D \leqslant 4.3$
Burning fuel characteristics	
Mass burning rate (for both fuels used): $m = 0.039$ kg/m^2 s	
Fuel density (at 20°C): $823 \leqslant \rho \leqslant 825$ kg/m^3	

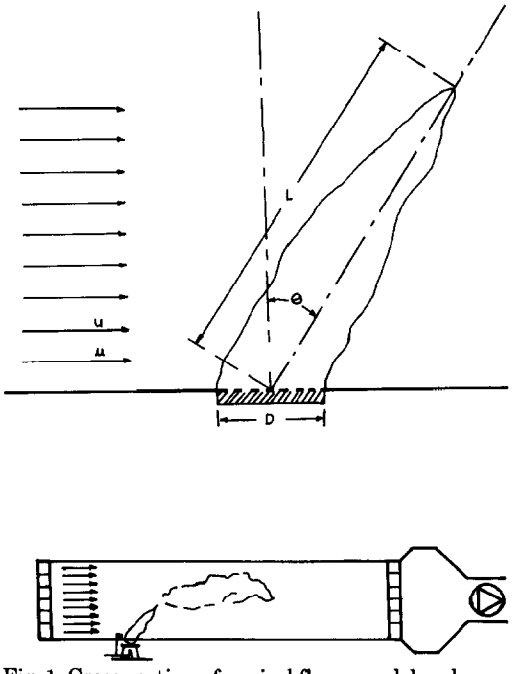

Fig. 1. Cross section of conical flame model and general view of wind tunnel.

near the bottom of wind tunnel, just over the edge of the burning pool (see u in Table 2), was estimated.

Flame length

Experimental data

Flame lengths were correlated with the pool diameters and the flame length-to-diameter dimensionless ratio was assessed for every burning pool. Such ratios are reported with wind speeds and other dimensionless numbers in Table 2.

Correlation of results

Still air experiments

In previous work [11] we determined the best-fit equation to the experimental data as

$$L/D = 32.3\left(\frac{m}{\rho_a\sqrt{gD}}\right)^{0.760} \quad . \tag{4}$$

TABLE 2

Flame length — Experimental data gathered with wind tunnel tests

L (m)	D (m)	(L/D)	u (m/s)	u^2/gD	$m/\rho_a\sqrt{gD}$ ($\times 100$)	$uD\rho_a/\mu_a$
0.257	0.109	2.35	0.000	0.000	3.19	0.000
0.200	0.0738	2.71	0.000	0.000	3.88	0.000
0.182	0.0600	3.03	0.000	0.000	4.20	0.000
0.147	0.0481	3.06	0.000	0.000	4.69	0.000
0.144	0.0437	3.30	0.000	0.000	4.92	0.000
0.263	0.108	2.44	0.250	0.0591	3.21	1734
0.195	0.0738	2.64	0.250	0.0863	3.88	1188
0.310	0.109	2.83	0.748	0.521	3.19	5268
0.225	0.0738	3.05	0.703	0.683	3.88	3342
0.200	0.0603	3.32	0.191	0.0617	4.19	770.8
0.173	0.0518	3.34	0.191	0.0718	4.52	662.1
0.150	0.0437	3.43	0.191	0.0851	4.92	558.6
0.165	0.0479	3.44	0.191	0.0776	4.70	612.3
0.215	0.0597	3.60	0.891	1.36	4.21	3560
0.164	0.0441	3.72	0.891	1.83	4.90	2630
0.190	0.0478	3.97	0.891	1.69	4.71	2850
0.157	0.0366	4.29	0.891	2.21	5.38	2182

Wind influence on flame length

Experimental data from the tests have been combined in Fig. 2 as L/D plotted against $(m/\rho_a\sqrt{gD})^5 \cdot (u^2/gD)^{-1} \cdot (uD\rho_a/\mu_a)$.

There are two points of interest in Fig. 2.

First, the dimensionless number $(m/\rho_a\sqrt{gD})$ has the most important role for predicting flame length.

Actually, by observing the data shown in Table 2 for wind runs, one can note that the flame length-to-diameter ratio increases even though the Froude number (u^2/gD) increases and the Reynolds number $(uD\rho_a/\mu_a)$ decreases. It is known that an increase of Froude number and a decrease of Reynolds number can cause a downward trend of flame length [5,11,12]. However, the dimensionless number $(m/\rho_a\sqrt{gD})$ also increases, increasing the flame length-to-diameter ratio. Thus it compensates the negative contribution of both Froude and Reynolds numbers.

The second point of interest in Fig. 2 is that there is a substantial difference between diffusion flames arising from pools with Froude numbers lower than 0.1 and those with Froude numbers higher than 0.1. In particular, the influence of the dimensionless number $(m/\rho_a\sqrt{gD})$ produces an increase of flame length-to-diameter ratio at large Froude numbers.

Bearing this in mind, the experimental data of wind tests have been split into two different groups depending on the Froude number, Fr (see Figs. 3 and 4).

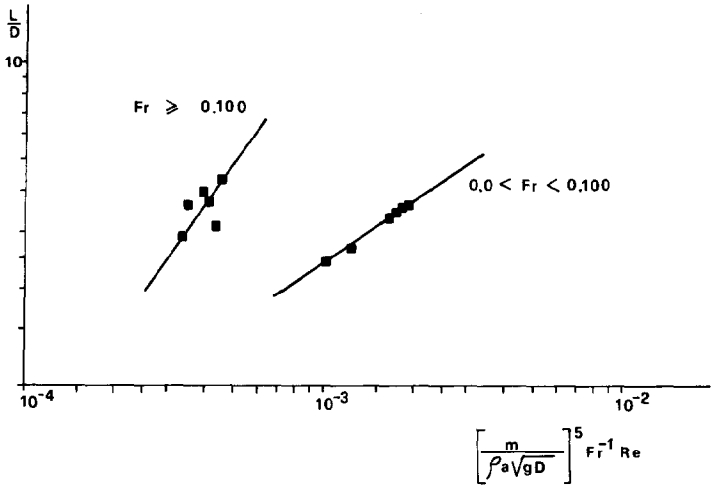

Fig. 2. Wind effectiveness on flame length. Difference between diffusion flames arising from burning pools with low Froude numbers and those ones arising from burning pools with high Froude numbers.

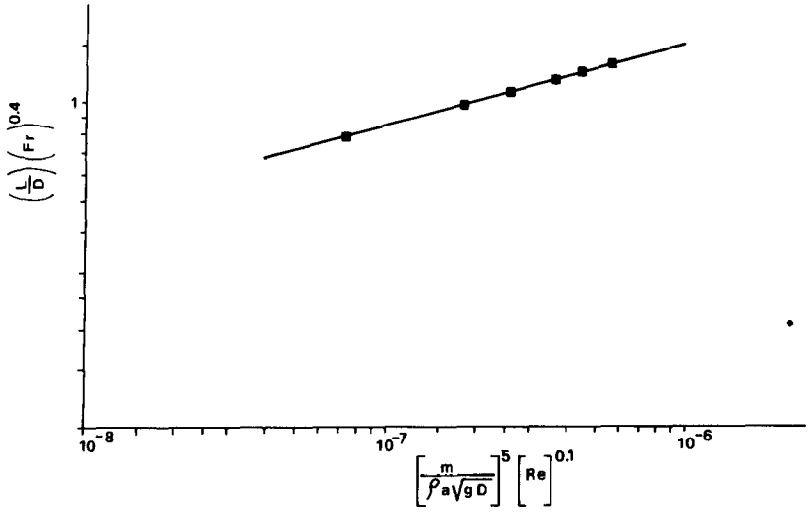

Fig. 3. Wind experiments. Diffusion flames arising from pools with low Froude numbers ($0.00 < Fr < 0.100$).

The experimental data for diffusion flames arising from pools with low Froude numbers (<0.1) have been plotted in Fig. 3 as $L/D \cdot (u^2/gD)^{0.4}$ against $(m/\rho_a\sqrt{gD})^5 \cdot (uD\rho_a/\mu_a)^{0.1}$. The most representative equation for experimental data plotted in Fig. 3 has been assessed to be

$$L/D = 43.4(m/\rho_a\sqrt{gD})^{1.22} \cdot (u^2/gD)^{-0.4} \cdot (uD\rho_a/\mu_a)^{0.0243} \quad , \qquad (5)$$

for $0 < Fr < 0.1$.

On the other hand, the experimental data of diffusion flames arising from pools with high Froude numbers ($\geqslant 0.1$) are shown in Fig. 4 as $(L/D)^{0.8} \cdot (u^2/gD)^{0.1} \cdot (m/\rho_a\sqrt{gD})^5$ plotted against $(m/\rho_a\sqrt{gD})^5 \times (uD\rho_a/\mu_a)^{0.5}$. The experimental data shown in Fig. 4 may be represented by:

$$L/D = 11.6(m/\rho_a\sqrt{gD})^{2.65} \cdot (u^2/gD)^{-0.125} \cdot (uD\rho_a/\mu_a)^{0.890} \quad , \qquad (6)$$

for $Fr \geqslant 0.1$.

Equations (5) and (6) show that Reynolds number effectiveness on the flame extent is greater for those flames arising from burning pools with high Fr than those arising from burning pools with low Fr. In other words eqns. (5) and (6) show that the flame length-to-diameter ratio is more strongly linked to the Reynolds number as the Froude number increases.

The maximum variation of experimental data shown in Fig. 4 from eqn. (6) is nearly 1%, while neglecting the Reynolds number (Re) contribution the maximum shift is nearly 10% [11].

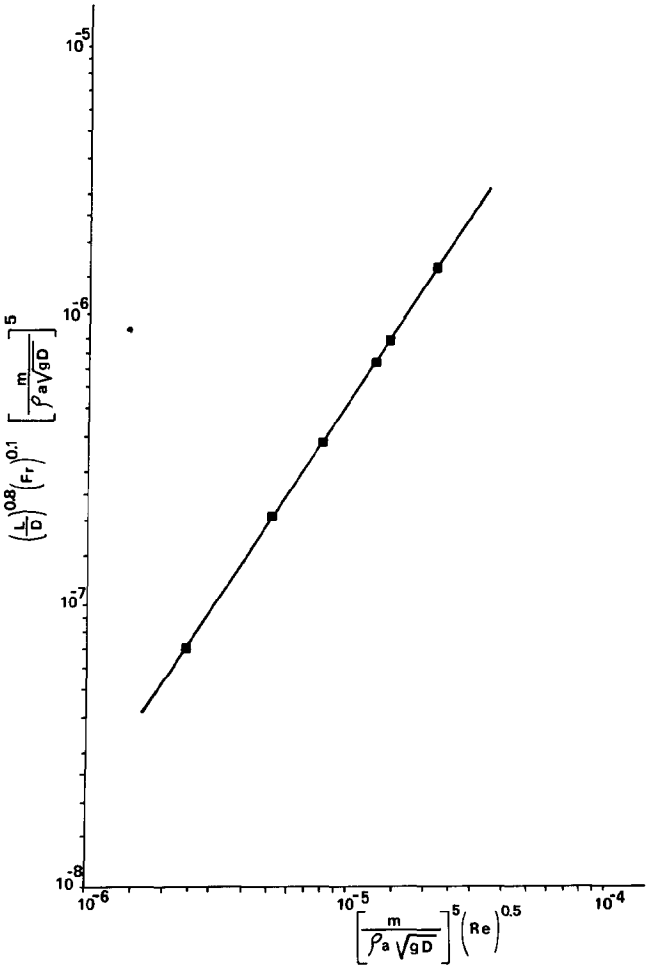

Fig. 4. Wind experiments. Diffusion flames arising from pools with high Froude numbers ($Fr \geqslant 0.100$).

Effect of wind on flame bending

Theoretical analysis

Sliepcevich developed a theoretical analysis [1] in order to derive an expression for the angle to which a flame is bent from the vertical by the wind.

Sliepcevich proposed the following general expression which applies for all flame shapes.

$$C_f(Re) = \frac{2f}{\beta}\left(1-\frac{\rho_f}{\rho_a}\right)\frac{\tan\theta}{Fr}\exp\left\{\left[1-\left(\frac{1}{D^*}\right)\right]k\right\} \quad , \tag{7}$$

where C_f (Re) is a "normalized" drag coefficient which is to be evaluated experimentally; f is a shape factor and β is a ratio of drag coefficients. Both variables depend upon flame geometry. D^* is a dimensionless diameter ratio $(D/D_{ref.})$ and k is an empirical constant evaluated to give the best fit of the data $(k=-2.2)$.

For instance, conical shaped flames were observed in the present experimental runs, therefore the parameter f assumes the value of $\pi/6$ [1] and β is defined as to be the drag coefficient of a cone at a particular angle of attack divided by the drag coefficient for the same cone with an angle of attack of 90°.

Values of β are always equal to or less than unity and may be obtained from several sources.

Those values shown in Table 3 have been derived from Streeter's Fig. 12II.22 [13] and have been plotted in Fig. 5 against $\cos\theta$ for $\cos\theta > 0.2$.

The best-fit equation to Fig. 5 has been calculated for conical shaped flames to be

$$\beta = (\cos\theta)^{1.38} \tag{8}$$

Sliepcevich proposed for his experimental data that k should assume the value of -2.2 [1].

For this study the above value of k has been adopted as well, because it provides the best fit to the present data.

The reference diameter $(D_{ref.})$ is the smallest diameter used in the experiments.

All of the variables necessary for the calculation of C_f (Re) were measured in the experimental runs reported in Table 3, except the average flame gas temperature which is required for the evaluation of the density ratio, ρ_f/ρ_a.

The density ratio may be calculated by the following expression by assuming ideal gas behaviour as $\rho_f/\rho_a = (T_a/T_f)\cdot(M_f/M_a)$. The assumption of ideal gas behaviour is a very good one. However, since M_f is approximately equal to M_a, the density ratio simply becomes

$$\rho_f/\rho_a = T_a/T_f \quad , \tag{9}$$

and by substituting eqns. (8) and (9) into eqn. (7) and assuming $f=\pi/6$ for conical shaped flames [1], we obtain for C_f

$$C_f\,(Re) = \frac{\pi}{3(\cos\theta)^{1.38}}\left[1-\left(\frac{T_a}{T_f}\right)\right]\cdot\left(\frac{\tan\theta}{Fr}\right)\exp\left\{\left[1-\frac{1}{D^*}\right)\right]k\right\} \quad . \tag{10}$$

By rearranging eqn. (10) in terms of angle of the flame tilt one obtains

$$\left[\frac{\tan\theta}{(\cos\theta)^{1.38}}\right] = \frac{(3/\pi)C_f(Re)\cdot Fr}{[1-(T_a/T_f)]\exp\{[1-(1/D^*)]k\}} \quad . \tag{11}$$

The dimensionless ratio $[\tan\theta/(\cos\theta)^{1.38}]$ in eqn. (11) represents an index of

TABLE 3

Flame bending – Results of wind tunnel tests

D (m)	u (m/s)	Fr	θ	$\tan\theta$	β	$1-T_a/T_f$	D^* [a]	$\exp\{[1-1/D^*]k\}$ [b]	$C_f(Re)$ [c]	Re	$C_f(Re)\cdot Fr$
0.0437	0.191	0.0851	41°80″	0.894	0.667	0.805	1.19	0.699	9.29	558.6	0.791
0.0479	0.191	0.0776	44°20″	0.972	0.632	0.805	1.31	0.595	9.93	612.3	0.771
0.0518	0.191	0.0718	43°90″	0.963	0.636	0.805	1.42	0.524	9.32	662.1	0.669
0.0603	0.191	0.0617	46°50″	1.05	0.598	0.805	1.65	0.421	10.1	770.8	0.625
0.0738	0.250	0.0863	45°90″	1.03	0.607	0.800	2.02	0.330	5.44	1188	0.470
0.108	0.250	0.0591	49°50″	1.17	0.551	0.800	2.94	0.234	7.04	1734	0.416
0.0738	0.703	0.683	59°60″	1.70	0.391	0.800	2.02	0.330	1.76	3342	1.20
0.109	0.748	0.521	58°40″	1.62	0.410	0.800	2.99	0.231	1.47	5268	0.768
0.0366	0.891	2.21	52°80″	1.32	0.500	0.805	1.00	1.00	1.00	2182	2.22
0.0441	0.891	1.83	54°80″	1.42	0.468	0.805	1.20	0.688	0.957	2630	1.76
0.0478	0.891	1.69	54°70″	1.41	0.470	0.805	1.31	0.597	0.893	2850	1.51
0.0597	0.891	1.36	59°10″	1.67	0.398	0.805	1.63	0.427	1.11	3560	1.51

[a] $D^* = (D/D_{ref.})$.
[b] $k = -2.2$
[c] Calculated from eqn. (10).

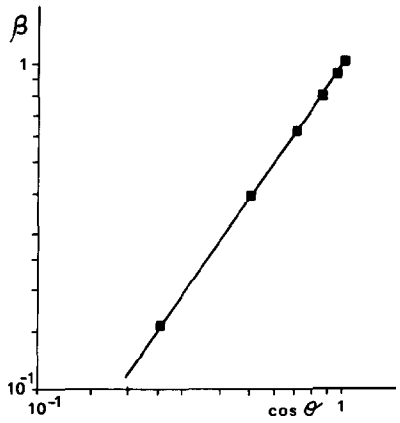

Fig. 5. Drag coefficient ratio (β) vs. cosθ for conical shaped flames.

TABLE 4

Dimensionless ratio $\tan\theta/(\cos\theta)^{1.38}$, and angle of flame tilt (θ) for cone-shaped flames

$\tan\theta/(\cos\theta)^{1.38}$	θ (deg.)
0	0
0.281	15
0.704	30
1.61	45
4.51	60
24.1	75
$+\infty$	90

flame bending. In fact, as shown in Table 4, if the angle of tilt increases, the above ratio will also increase. Equation (11), which has been derived from the general expression, eqn. (7), proposed by Sliepcevich's theoretical analysis [1], shows the explicit dependence of the flame bending with Froude and Reynolds numbers.

Experimental data

Diffusion flames arising from burning pools of liquid hydrocarbon were observed in wind tunnel experiments to determine the extent of bending by wind. The method adopted for measuring the angle of the tilt, due to wind, is illustrated in the paragraph concerning wind tunnel experiments.

Experimental results are recorded in Table 3 along with other calculated data. Bearing in mind eqn. (11) and in order to visualize the flame bending dependence on Reynolds number, experimental data gathered in Table 3 have

been combined in Fig. 6 as $[C_f(Re)Fr]$ against Reynolds number, the dimensionless parameter $C_f(Re)$ has been calculated by means of eqn. (10). There are two points worth noting in Fig. 6. First, the angle of tilt decreases as Reynolds number rises, this result is in accordance with Sliepcevich's paper [1]. Second, there is a substantial difference between burning pools with high Froude numbers and those with small Froude numbers. For a given Reynolds number the flame tilt increases as the Froude number increases.

Since our objective is to find a method for predicting the behaviour of large flames, it is of interest to explore the suitability of eqn. (11) in the limit as the diameter becomes large.

By applying eqn. (11) for large diameters one finds that

$$\left[\frac{\tan\theta}{(\cos\theta)^{1.38}}\right]=\frac{3C_f(Re)\cdot Fr}{\pi e^{-2.2}(1-T_a/T_f)} \tag{12}$$

for conical shaped flames.

Equation 12 is similar to Sliepcevich's expression for calculating the angle of flame tilt [1] except for its treatment of the drag coefficient ratio (β) and approximation for $(1-\rho_f/\rho_a)$.

The aim of the present study is to derive from Sliepcevich's theoretical anal-

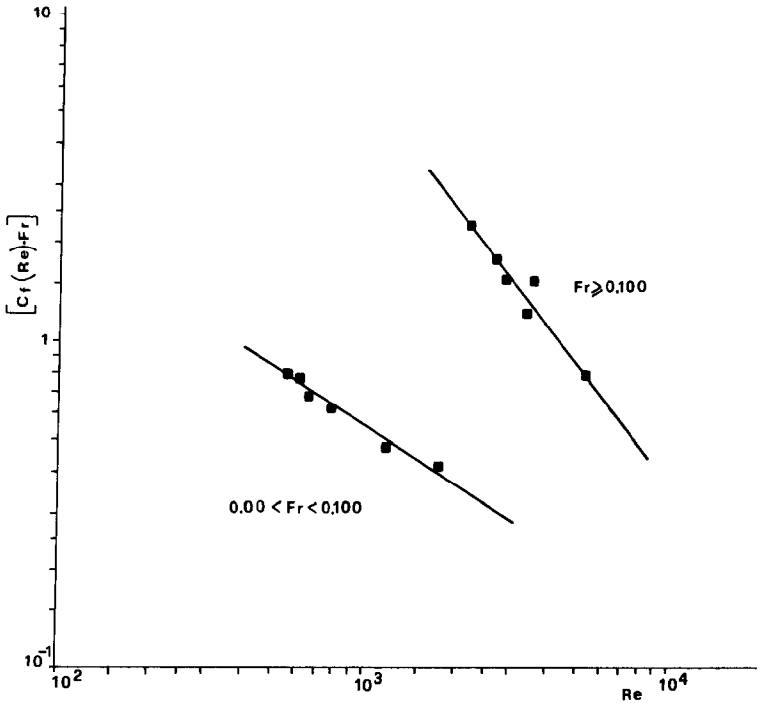

Fig. 6. Variation of flame bending index with Reynolds number for diffusion flames arising from burning pools of liquid. Conical shaped flames.

ysis simple and practical equations for predicting flame angle of tilt due to the wind for conical and cylindrical shaped flames.

Though the correlating expression of eqn. (11) at large diameters reduces to the rather simple expression in eqn. (12), the use of eqn. (12) is limited by the uncertainty in extrapolation of $C_f(Re)\cdot Fr$ values from Fig. 6 for large Reynolds numbers.

Sliepcevich observed that, from almost casual observation of large scale flames, one can say with certainty that an extrapolation is not valid.

However, observing a few uncontrolled fires up to 6 m in diameter, Sliepcevich suggested that at large Reynolds numbers the "normalized" drag coefficient C_f (Re) may approach unity [1], so that the dimensionless ratio $[\tan\theta/(\cos\theta)^{1.38}]$ is approximated by the following expression which is derived directly from eqn. (12):

$$\left[\frac{\tan\theta}{(\cos\theta)^{1.38}}\right]=8.62\left\{\frac{Fr}{(1-T_a/T_f)}\right\}, \tag{13}$$

for large diameters and conical shaped flames.

By applying eqn. (13) and using Table 4, one is able to measure the angle of tilt, due to the wind, of conical shaped flames rising from large burning pools of liquid.

Bending aspect of cylindrical flames

By altering eqn. (7) for cylindrical shaped flames with large diameters, where $f=\pi/4$ [1] and the drag coefficient ratio β may be derived from Streeter's Fig. 12II.7 [13] to be $(\cos\theta)^{0.515}$, one finds that

$$\left[\frac{\tan\theta}{(\cos\theta)^{0.515}}\right]=5.75\left\{\frac{Fr}{(1-T_a/T_f)}\right\}. \tag{14}$$

TABLE 5

Dimensionless ratio $\tan\theta/(\cos\theta)^{0.515}$ and angle of flame tilt (θ) for cylindrical flames

$\tan\theta/(\cos\theta)^{0.515}$	θ (deg.)
0	0
0.273	15
0.622	30
1.20	45
2.48	60
7.49	75
$+\infty$	90

By applying eqn. (14) and using the figures shown in Table 5, one is able to measure with a good approximation the angle of flame tilt, due to wind, of cylindrical shaped flames arising from large burning pools of liquid.

Conclusions

The aim of this paper is to present a single systematic study of the wind effect on diffusion flames of fires of high source momentum ($Q^* > 1$).

The results presented in this paper show that the length of the diffusion flames of fires with high source momentum is strongly affected, not only by the source Froude number, but also by the source Reynolds number, particularly if the Froude number exceeds 0.1.

On the other hand, the Reynolds number contribution on flame length is negligible if the Froude number is less than 0.1.

The experimental data gathered in this study also suggest the following relationship:

$L/D \sim 0.65\, Q^*$, for $3.8 < Q^* < 6.7$.

Moreover, two simple and practical equations for predicting the flame angle of tilt due to wind for conical and cylindrical shaped flames with large diameters have been presented.

These expressions show that flame bending by wind is strongly linked with the source Froude number, and this brings about an increase in the angle of flame tilt depending on flame shape.

Notation

$C_f\,(Re)$	Normalized drag coefficient, eqn. (7) (dimensionless)
C_p	Specific heat of air at constant pressure, kJ/kg K (at ambient temperature = 1.005 kJ/kg K)
D	Diameter of the burning pool, flame diameter, m
D^*	Dimensionless diameter ratio, $D/D_{ref.}$
$D_{ref.}$	Reference diameter, m
f	Flame shape factor, eqn. (7) (dimensionless)
Fr	Froude number, u^2/gD (dimensionless)
g	Gravitational acceleration, m/s^2
k	Empirical constant, eqn. (7) (dimensionless)
L	Flame length, m
L/D	Flame length-to-diameter dimensionless ratio
m	Mass burning rate. See Table 1, kg/m^2s
$m/\rho_a\sqrt{gD}$	Dimensionless number, eqn. (4)
M	Molecular weight, kg/kmol

p	Power representing flame shape and describing flame length. See eqn. (2) (dimensionless)
Q	Heat release rate assuming efficient combustion, kJ/s (kW)
Q^*	Dimensionless ratio. See eqn. (1)
R	Gas constant, J/mol K
Re	Reynolds number, $uD\rho_a/\mu_a$ (dimensionless)
Re_L	Flame-tip Reynolds ratio, estimated by eqn. (3) (dimensionless)
T	Temperature, K
u	Wind speed, m/s

Greek symbols

β	Drag coefficient ratio (dimensionless)
θ	Bending angle of flame from the vertical, angle of flame tilt (dimensionless)
μ	Dynamic viscosity, kg/m s
ν	Kinematic viscosity, m^2/s
ρ	Density, kg/m^3

Subscript symbols

a	Surrounding air
f	Flame

References

1 C.M. Sliepcevich and O.A. Pipkin, Effect of wind on buoyant diffusion flames, Ind. Eng. Chem., Fundam., 3(2) (1964) 147-154.
2 E.E. Zukoski, T. Kubota and B. Cetegen, Fire Saf. J., 3 (1980/81) 107.
3 P.H. Thomas, C.T. Webster and M.M. Raftery, Some Experiments on buoyant diffusion flames, Combust. Flame, 5 (1961) 359-367.
4 G. Cox and R. Chitty, A study of the deterministic properties of unbounded fire plumes, Combust. Flame, 39 (1980) 191-209.
5 H.A. Becker and D. Liang, Visible length of vertical free turbulent diffusion flames, Combust. Flame, 32 (1978) 115-137.
6 P.K. Raj, Am. Soc. Mech. Eng. Paper 81-HT-17, 1981 (report).
7 G. Cox and R. Chitty, Some source-dependent effects of unbounded fires, Combust. Flame, 60 (1985) 219-232.
8 G. Heskestad, Fire Saf. J., 5 (1983) 103.
9 B.M. Cetegen, E.E. Zukoski and T. Kubota, NBS-GCR-82 (1982) 402.
10 V.I. Blinov and G.N. Khudiakov, Dokl. Akad. Nauk SSSR, 113 (1957) 1094; reviewed by H.C. Hottell, Fire Res. Abstr. Rev., 1 (1959) 41.

11 D.M. De Faveri, A. Vidili, E. Palazzi, C. Zonato and G. Ferraiolo, Effect of wind on thermal radiation of flames in uncontrolled, and large, combustion - Preliminary study, in: Proc. XIth World Congress on the Prevention of Occupational Accidents and Diseases, Stockholm, May 1987.
12 P.H. Thomas, The size of flames from natural fires, in: Ninth Symp. on Combustion, Cornell Univ., Ithaca, NY. Academic Press, New York, NY, 1963, pp. 844–859.
13 V.L. Streeter, Handbook of Fluid Dynamics. McGraw-Hill, New York, NY, 1961.